J. Res. Technol. Eng. 7(1), 2026, 157-172

Journal of Research Technology and Engineering
www.jrte.org

Rational Design of Trametinib Analogues for MEK1 Inhibition: An In Silico Approach

A.S.Weerasekara[1], *S.S.Uthumange[1]

[1]Faculty of Science, NSBM Green University
*sahani.u@nsbm.ac.lk

Received: 25 November 2025; Revised: 20 December 2025; Accepted: 22 December 2025; Available online: 10 January 2026

Abstract: Trametinib, a selective MEK inhibitor, is widely used in the treatment of several cancers. This study aimed to design trametinib analogues with enhanced MEK1 inhibition using an *in silico* strategy. Structural modifications to the trametinib scaffold were explored through molecular docking. A library of 34 compounds was assessed, among which compounds 1C and 2R demonstrated more favorable binding energies (-12.93 kcal/mol and -13.08 kcal/mol, respectively) than trametinib (-12.00 kcal/mol). These two candidates were therefore selected for further analysis. Molecular dynamics simulations showed that 1C and 2R formed more stable interactions with key MEK1 residues, SER212, VAL127, and PHE209, compared to the parent drug. The analogues were further evaluated using computational pharmacokinetic and drug-likeness profiling. The lead compound, 2R, exhibited an overall efficacy profile superior to trametinib. These findings provide a strong rationale for future synthetic and biological studies aimed at improving therapeutic outcomes in MEK1-driven cancers.

Index Terms: Drug Discovery, Molecular Docking, MEK1 inhibition, Trametinib

1 Introduction

The transduction of extracellular signals into cellular responses is significantly dependent upon the mitogen-activated protein kinase (MAPK) signalling cascade [1]. MEK represents a pivotal regulatory point in the RAS-RAF-MEK-ERK mitogen-activated protein kinase (MAPK) signalling pathway [2]. A notable characteristic of many human cancers is the dysregulation of the Raf/MEK/ERK protein kinase cascade, a three-tiered signalling pathway, which is predominantly driven by oncogenic alterations in RAF, RAS, or cell surface receptor tyrosine kinases [1]. Two distinct isoforms of MEK, MEK1 and MEK2, are present in the human proteome. Despite differences in their primary sequence, with a 79% identity, these isoforms show functional equivalence in the phosphorylation of specific tyrosine and threonine residues in ERK substrates [3]. Augmented MEK activity precipitates aberrant activation of the RAS-RAF-MEK-ERK signalling cascade, a pathway implicated in the pathogenesis of inflammatory conditions and approximately 30% of human malignancies [4].

Trametinib, a pharmaceutical used in cancer treatment, operates by suppressing the enzymatic activity of mitogen-activated protein kinase 1 (MEK1) and MEK2 [5]. Contrary to a deliberate search for MEK inhibitors, the development of trametinib arose from an unanticipated observation derived from a phenotypic high-throughput screen that detected compounds capable of increasing $p15^{INK4b}$ expression [6]. In 2013, trametinib (GSK1120212, JTP74057) received FDA approval as a standalone treatment for adult individuals diagnosed with melanoma harbouring BRAF V600E or V600K mutations [7]. Japan Tobacco was the original developer of the compound, for which GlaxoSmithKline subsequently secured exclusive worldwide licensing

rights [7]. Trametinib's bioavailability facilitates its oral administration [8].

Ligand binding to MEK occurs at two separate sites, categorized as the allosteric and ATP-binding sites [9]. As an allosteric inhibitor, trametinib targets MEK 1/2. This mode of inhibition is important as it enables trametinib to exhibit a high degree of specificity for MEK 1/2, thereby decreasing the risk of interference with other enzymatic processes and related side effects [10]. Also, the interaction profiles of MEK1 and MEK2 demonstrate a marked concordance [11]. The classification of trametinib as a type III allosteric MEK1 inhibitor is attributed to its binding in a region juxtaposed to the ATP-binding pocket [12].

Beyond its original application in melanoma, trametinib is presently being investigated and utilized as a therapeutic agent for a variety of cancers, including non-small cell lung cancer [13], anaplastic thyroid cancer [14], and glioma [15]. Although trametinib has shown therapeutic advantages, its use is accompanied by the potential for adverse events. A phase 2 basket trial examining the dabrafenib-trametinib regimen identified 3 chills, nausea, pyrexia, rash, and fatigue as the most common treatment-related adverse occurrences [16]. An emergence of trametinib resistance, with clinical significance, has also been observed. To combat resistance and improve cancer treatment, studies investigate MEK1/2 inhibitor combination therapies [17]. The search for new inhibitors is crucial to resolve these problems, and in this context, computational *in silico* methods provide an advantageous early discovery strategy.

The purpose of this research was to analyze and characterize potential trametinib analogues, with the goal of selecting compounds possessing enhanced MEK1 binding affinity, refined interaction profiles, and optimized pharmacokinetic properties in comparison to the parent drug. The insights gained from this research contribute to the advancement of computational drug discovery strategies for MEK inhibition, facilitating the development of next-generation cancer therapies.

2 MATERIALS AND METHODS

As shown in Fig. 1, modifiable functional groups in trametinib were identified through literature and replaced with appropriate bioisosteres. In the pursuit of this, a compound library with 34 derivatives was made (Fig. 2).

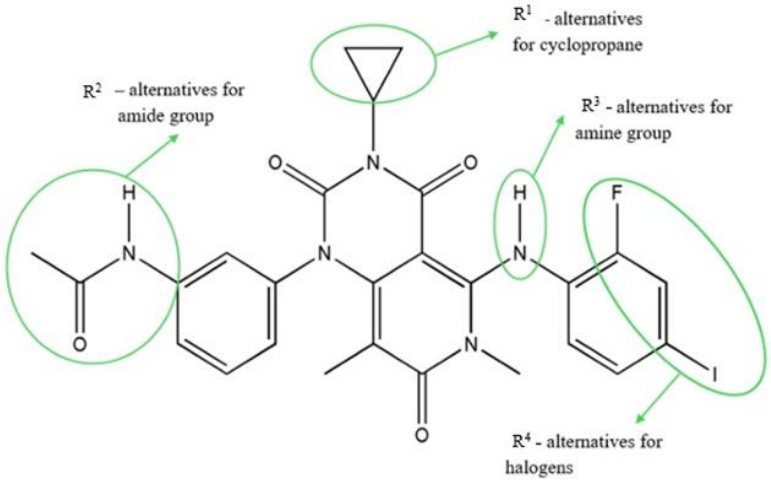

Fig. 1 - Structure of trametinib with modifiable functional groups. The regions labelled R^1, R^2, R^3, and R^4 indicate positions where structural modifications can be made, including alternatives for the cyclopropane (R^1), amide group (R^2), amine group (R^3), and halogen substitutions (R^4).

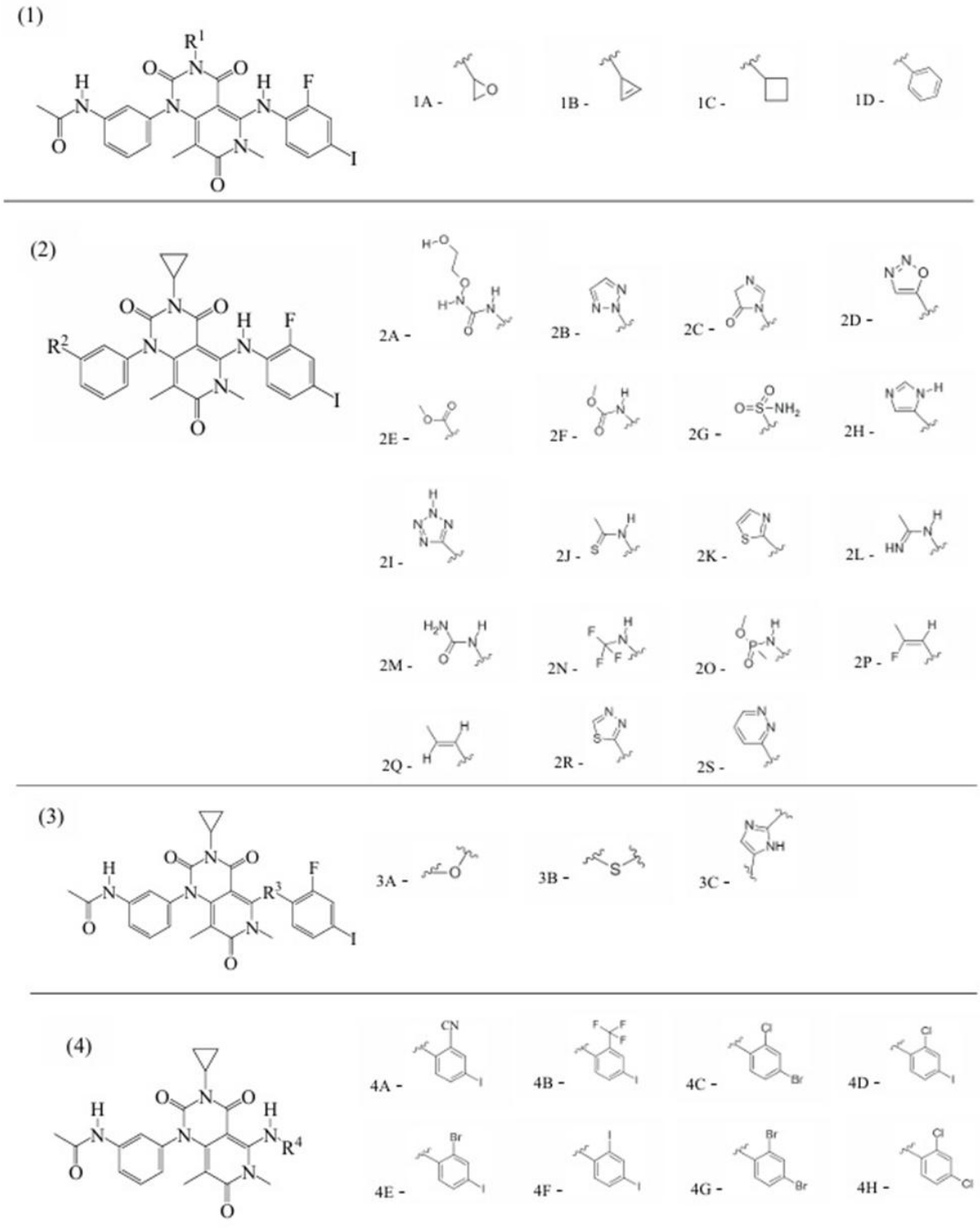

Fig. 2 - Analogues with modifications at the R^1, R^2, R^3, R^4 positions

2.1 Docking Process

A docking process was then conducted to screen the library of compounds to identify the best compound for use in place of trametinib. Autodock 4.2.6 software was employed, integrated with Chemdraw and Chem3D

software tools [18]. The docking process was divided into 2 parts: enzyme preparation and ligand preparation.

2.1.1 Enzyme preparation

The MEK1 protein's initial structural coordinates were obtained from the Protein Data Bank (PDB ID – 4ARK) [19]. The protein structure, after removal of redundant residues, water molecules, and extraneous chains, was prepared for AutoDock input by incorporating polar hydrogen atoms, repairing missing atoms, assigning Kollman charges, and saving the structure in PDBQT format.

2.1.2 Ligand preparation

Ligand preparation entailed initial generation and minimization of energy using ChemDraw and Chem3D, followed by optimization and conversion to PDBQT format for AutoDock, which involved the addition of hydrogen atoms and Gasteiger charge assignment, ensuring compatibility for docking simulations. The grid box parameters (x-33.469, y-26.668, z-39.334) were precisely defined based on the ligand's centre coordinates and size. The control docking experiment produced a low root-mean-square deviation (RMSD), thereby validating the reliability of the established protocol. With the protocol validated, the docking procedure was then performed across the entire compound library. The binding energy and inhibition constant values for each compound were obtained. Three compounds, characterized by the most optimal binding energies, were chosen for further evaluation.

2.2 Simulation studies

VMD 1.9.3 software [20] and Biovia Discovery software were utilized to visualize the selected compounds and the control, trametinib. A comprehensive interaction profile was generated, illustrating the distinct bonds and interactions between each ligand and the MEK1 protein.

2.3 Subsequent validation docking protocol

Further control docking experiments were implemented to validate the stability and reproducibility of the crucial binding site interactions. A comparative re-docking study was conducted across several high-quality MEK1 PDB entries using their respective co-crystallized ligands. Ligands chosen for the re-docking were structurally and mechanistically similar to trametinib to confirm that the chosen protein conformer was optimized for this specific inhibitory class. The study utilized a set of well-established MEK1 inhibitors, including trametinib, selumetinib, and mirdametinib, as the test ligands (Table 1) [21]. Molecular interactions were analyzed and visualized using Biovia Discovery software.

Table 1 - MEK1 complexes and their various ligand partners

PDB ID of MEK1 complexes	Ligands
7JUR	Trametinib
7JUU	Mirdametinib
7JUZ	Selumetinib

2.4 Pharmacokinetic evaluation

A pharmacokinetic assessment was conducted for the selected compounds, utilizing the SWISSADME [22] and pkCSM [23] applications. This evaluation aimed to assess and validate the drug-like properties of each compound, with the optimal compound determined through a combined analysis of interaction profiles and pharmacokinetic data.

3 RESULTS AND DISCUSSION

3.1 Docking results

According to the results of Table 2, compound 1D possessed the highest binding energy, with compounds 2R and 1C ranking second and third, respectively.

Table 2 – Estimated free binding energy values and estimated inhibition constant (Ki) values of all the compounds that were used in the docking process

Compound name	Estimated free energy of binding	Estimated inhibition constant (Ki)
Trametinib	**-12.00 kcal/mol**	**1.60 nM**
1A	-12.09 kcal/mol	1.38 nM
1B	-12.13 kcal/mol	1.28 nM
1C	**-12.93 kcal/mol**	**332.16 pM**
1D	-13.86 kcal/mol	69.25 pM
2A	-11.21 kcal/mol	6.09 nM
2B	-11.12 kcal/mol	7.08 nM
2C	-12.67 kcal/mol	515.11 pM
2D	-12.70 kcal/mol	488.17 pM
2E	-11.66 kcal/mol	2.86 nM
2F	-11.19 kcal/mol	6.25 nM
2G	-11.64 kcal/mol	2.92 nM
2H	-12.55 kcal/mol	631.30 pM
2I	-11.99 kcal/mol	1.64 nM
2J	-12.38 kcal/mol	836.43 pM
2K	-11.84 kcal/mol	2.08 nM
2L	-10.87 kcal/mol	10.81 nM
2M	-11.67 kcal/mol	2.77 nM
2N	-11.10 kcal/mol	7.27 nM
2O	-10.71 kcal/mol	14.23 nM
2P	-11.25 kcal/mol	5.68 nM
2Q	-11.65 kcal/mol	2.89 nM
2R	**-13.08 kcal/mol**	**259.99 pM**
2S	-12.70 kcal/mol	492.02 pM
3A	-12.43 kcal/mol	767.73 pM
3B	-10.54 kcal/mol	18.87 nM
3C	-11.80 kcal/mol	2.25 nM
4A	-12.09 kcal/mol	1.38 nM
4B	-12.38 kcal/mol	845.43 pM
4C	-12.10 kcal/mol	1.34 nM
4D	-12.48 kcal/mol	710.86 pM
4E	-12.78 kcal/mol	430.15 pM

4F	-11.17 kcal/mol	6.46 nM
4G	-11.39 kcal/mol	4.51 nM
4H	-11.53 kcal/mol	3.52 nM

The foundational structure of trametinib, as observed in its early discovery phase, presented three aromatic rings integrated within a pyridopyrimidine core (similar to 1D compound), nevertheless, the elevated hydrophobicity of it led to the strategic replacement of the N-3 phenyl substituent with a bioisosteric cyclopropyl ring, chosen to increase polarity [11]. Therefore, despite its high binding energy, compound 1D was excluded from further analysis. The final set of compounds selected for detailed study included 1C, 2R, and trametinib. A comprehensive interaction profile analysis was then conducted for these selected compounds.

3.2 Interaction profile analysis

To better understand the binding behavior and molecular interactions of the selected compounds, an in-depth interaction profile analysis was performed. In trametinib, among the three hydrogen bonds that were visualized, two were formed with the amide group of trametinib (Fig. 3A). An important pi-pi stacking interaction was also observed with PHE209. Analysis of the trametinib-MEK1 complex revealed additional interactions involving iodine atoms and the residues CYS207, MET143, and VAL127. A significant electrostatic interaction with VAL127 (4.29 Å) was also identified.

Compound 2R, with a 1,3,4-thiadiazol substituent at the R^2 position, was found to have the strongest binding energy in the series. Two essential hydrogen bonds with VAL211 and SER212 were observed in 2R (Fig. 3C). Importantly, 2R also forms halogen interactions with the target protein, utilizing iodine and fluorine atoms to interact with VAL127, CYS207, ASP208, and MET143. Additionally, pi-pi stacking with PHE209 was observed. A notable electrostatic interaction with VAL127 (4.16Å) was also detected.

The 1C compound was generated by substituting the cyclopropane ring in trametinib with a cyclobutane ring. Hydrogen bonds were observed with ARG234, LYS97, VAL211, and SER212 residues (Fig. 3B). The presence of a crucial electrostatic interaction with VAL127 (4.24Å) was established. Furthermore, a pi-pi stacking interaction with PHE209 was identified. The 1C compound forms also interactions with VAL127, MET143, and CYS207 using an iodine atom.

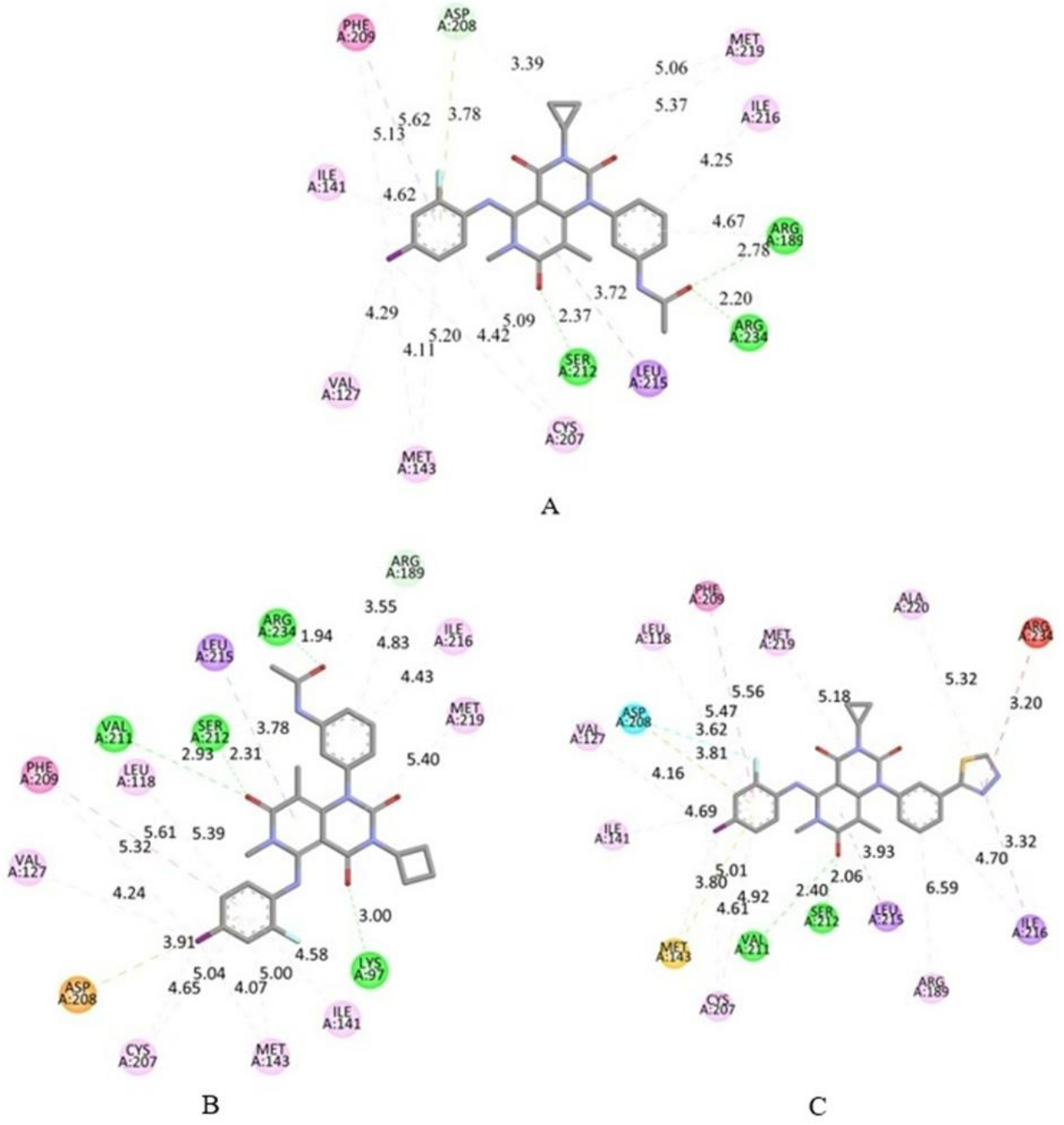

Fig. 3 – Interaction profile of (A) trametinib, (B) 1C, and (C) 2R in the active site of MEK1 (PDB ID – 4ARK)

Table 3 presents a comparative dataset of hydrogen bond formation, showing the distances of identified hydrogen bonds in trametinib relative to compounds 2R and 1C. While 1C more closely approximates trametinib's hydrogen bond distances overall, particularly at ARG234 and SER212, 2R demonstrates notably stronger interactions at residues deemed critical for allosteric binding. Orhen et al. [4] highlighted that stable interactions at VAL127 (electrostatic), SER212 (hydrogen bond), and PHE209 (pi-pi stacking) are critical, as they directly influence the inhibitory potency of a compound. Compound 2R demonstrates notably stronger hydrogen bonding with SER212 compared to both trametinib and 1C (see Table 3). Additionally, 2R exhibits

the most robust electrostatic interaction with VAL127 (4.16 Å) among the three compounds. Pi-pi stacking with PHE209 is also retained at 5.56 Å, slightly shorter than trametinib's 5.62 Å, indicating a maintained stabilizing interaction. In this context, the enhanced interactions observed in 2R suggest that it is likely the superior analogue, despite 1C maintaining a closer overall hydrogen bond network to trametinib.

Table 3 - Comparison of key hydrogen bond interactions between trametinib, 2R, and 1Cs.

Hydrogen bonds observed in trametinib	Trametinib	2R	1C
ARG234	2.20 Å	-	1.94 Å
SER212	**2.37 Å**	**2.06 Å**	**2.31 Å**
VAL211	-	2.40 Å	2.93 Å
LYS97	-	-	3.00 Å
ARG189	2.78 Å	-	-

Subsequently, further simulation studies were conducted among multiple MEK1 structures to investigate and validate the importance of various bonds that were observed in trametinib, 2R, and 1C with the MEK1 protein. PHE209 is the most frequently participating residue, forming pi-pi stacking interactions in all of the structures analyzed, demonstrating a high level of structural conservation for this specific interaction across various conformations. Also, SER212 exhibits hydrogen bonding in all PDB structures, establishing it as the most frequently participating residue (Table 4).

The PDB entries 7JUU, 7JUR, and 7JUZ provide a structural basis for comparing the binding of distinct small-molecule ligands within the KSR-MEK1 protein complex (Table 4). The KSR-MEK1 complex was selected as the structural model for drug targeting because it represents a physiologically relevant state of MEK1 when associated with its key regulators, KSR and RAF. The consistent presence of a measurable halogen bond at VAL127 indicates that this interaction plays a stable, structurally significant role in binding or conformation across different MEK1 states (Table 4).

Table 4 – Interactions with PHE209, SER212, and VAL127 across multiple allosteric MEK1 inhibitors

	7JUR (Trametinib)	7JUU (Mirdametinib)	7JUZ (Selumetinib)
PHE209	5.55 Å	5.34 Å	5.41 Å
SER212	2.20 Å	2.23 Å	3.47 Å
VAL127	4.49 Å	4.76 Å	4.62 Å

The maintenance of interactions with SER212, VAL127, and PHE209 by multiple allosteric MEK inhibitors (e.g., Trametinib, Mirdametinib, and Selumetinib) highlights the functional importance of these specific amino acids in mediating the inhibitory binding mechanism and defining the pharmacological activity of this class of compounds. Comparative structural analysis showed that 2R exhibited the strongest interactions with SER212 and VAL127 across all examined complexes of both free MEK and KSR-MEK1.

Contrary to ATP-site binding, most MEK inhibitors described in the literature exhibit binding to a pocket

positioned between the N- and C-terminal domains [24]. Another 22 important findings stated that the formation of a tertiary complex between the MEK enzyme, the ATP-binding site, and the inhibitor characterizes allosteric MEK1/MEK2 inhibitors, which are notable for their discriminating kinase inhibitory activity and uncompetitive inhibition [25]. Also, allosteric pockets, located in the vicinity of the αC helix and the ATP-binding site, are the exclusive binding targets for type III inhibitors [26]. Furthermore, in a previous computational analysis, CAVER 3.0 was employed to identify and characterize the pathways leading to the ATP-binding site and the allosteric binding site within the MEK protein models [2]. The binding site utilized by type III kinase inhibitors, located adjacent to the ATP-binding region, imparts significant target enzyme specificity. It is postulated that homologous allosteric pockets, similar to the 'MEK pocket,' may exist in other kinase enzymes, thereby offering opportunities for the design of related inhibitors [27].

It has been established through prior research that the benzene ring of PD184352, substituted with fluorine and iodine, occupies a nonpolar binding pocket in the MEK enzyme, formed by the amino acid residues MET143, ILE141, LEU118, and PHE209 [4]. The simulation data indicated that trametinib, consistent with PD184352, establishes diverse interactions with the aforementioned amino acid residues within a shared hydrophobic cavity. The capacity of halogens to participate in potent and selective non-covalent interactions has gained increasing recognition and significance within the domain of pharmaceutical research and development [28]. Additionally, Ohren et al. [4] revealed that diaryl amines engaged in crucial interactions with MEK residues, and, more specifically, the 2-fluoro-4-iodobenzene moiety exhibited several short-range contacts within a deeply recessed hydrophobic protein cavity. Among these short-range contacts, a key electrostatic interaction is formed between the VAL127 backbone carbonyl oxygen and the 4-iodine atom [4], as also observed in the compounds investigated in this study.

As previously reported, Ohren et al. [4] emphasized that in developing potent MEK1 inhibitors, compounds with strong interactions at VAL127, SER212, and PHE209 were prioritized, as these residues are crucial for allosteric binding and directly influence inhibitory potency. This finding was later supported by Zou et al. [29], who confirmed the importance of these interactions for maintaining high inhibitory activity. In the present study, comparable key interactions were identified, with compound 2R showing particularly strong binding to SER212 and VAL127, along with the highest binding energy among the series.

To further support the suitability of 2R as an alternative to trametinib, a computational alignment of their molecular structures was performed using VMD software (Fig. 4)

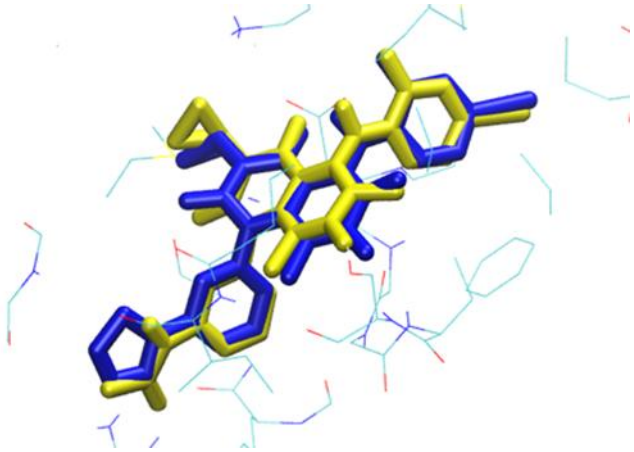

Fig. 4 – Visual representation of the structural comparison between compound 2R, represented in blue, and trametinib, represented in yellow.

By analyzing the superimposed structures, it demonstrates a high degree of overlap between the blue (2R) and yellow (Trametinib) molecules. This close overlap indicates a strong structural similarity, suggesting that 2R and Trametinib adopt similar conformations and potentially interact with biological targets comparably. Based on the interaction profile, it can be inferred that a congruent mechanism of action is operative.

3.3 Pharmacokinetic evaluation results

The integrated data derived from SWISSADME and pkCSM are detailed in Table 5.

Table 5 - Results of pharmacokinetic evaluation

		Trametinib	1C	2R
Molecular properties	**Molecular weight**	615 g/mol	629 g/mol	642 g/mol
	Chemical formula	$C_{26}H_{23}FIN_5O_4$	$C_{27}H_{25}FIN_5O_4$	$C_{26}H_{20}FIN_6O_3S$
	Surface area	223.238	229.603	231.902
Physicochemical properties	**Lipophilicity (LogP)**	3.82	4.11	4.36
	TPSA (Topological Polar SurfaceArea)	107.13 A^2	107.13 A^2	132.05 A^2
	Molar refractivity	149.59	154.39	154.18
	Bioavailability score	0.55	0.55	0.55

Druglikeness	**Lipinski's rules**	Yes; 1 violation: MW>500	Yes; 1 violation: MW>500	Yes; 1 violation: MW>500
	Synthetic accessibility	4.11	4.11	4.04
Absorption	**Water solubility**	-4.081 (log mol/L)	-4.145 (log mol/L)	-3.495 (log mol/L)
	Skin permeability	Low	Low	Low
	Intestinal absorption	91.063%	91.895%	100%
Distribution	**VDss (volume of distribution at steady state)**	0.172 (log L/kg)	0.228(log L/kg)	0.228(log L/kg)
	Fraction unbound	0.142 (Fu)	0.136 (Fu)	0.273 (Fu)
	BBB Permeability	-0.863 (log BB)	-0.841 (log BB)	-1.298 (log BB)
	CNS Permeability	-2.389 (log PS)	-2.297 (log PS)	-3.345 (log PS)
Metabolism	**CYP1A2 inhibition**	No	No	No
	CYP2C9 inhibition	Yes	Yes	Yes
	CYP2D6 inhibition	No	No	No
Excretion	**Total clearance**	-0.82 (log ml/min/kg)	-0.858 (log ml/min/kg)	-0.643 (log ml/min/kg)
Toxicity	**LD50 (Lethal Dose)**	3.285 (mol/kg)	3.297 (mol/kg)	3.179 (mol/kg)
	LOAEL (Oral Rat Chronic Toxicity)	0.653 (log mg/kg_bw/day)	0.522 (log mg/kg_bw/day)	0.118 (log mg/kg_bw/day)

Leonowens et al. [8] defined trametinib's pharmacokinetic properties, noting its moderate to high oral bioavailability, reduced first-pass metabolism, and extended terminal elimination, which collectively emphasize the drug's effective systemic absorption and its ability to achieve sustained therapeutic levels.

As a fundamental principle in molecular design, drug-likeness provides medicinal chemists with a framework to inform structural modifications during the stages of identifying initial hits and optimizing lead compounds [30]. According to Table 5, despite similar bioavailability profiles, Trametinib, 1C, and 2R share a common violation of Lipinski's Rule of Five, specifically exceeding the molecular weight threshold of 500, which may compromise their oral absorption and overall drug-like characteristics. Nevertheless, a research investigation

confirmed that upon the oral administration of a 2 mg dose of trametinib, the median time required to achieve maximum plasma concentration (t_{max}) was measured as 1.5 hours, and the mean effective elimination half-life ($t_{1/2}$) was approximately 4 days [31]. Compounds exhibiting violations of two or more of Lipinski's rules are generally recommended for exclusion from subsequent developmental stages [32]. In contrast, a separate investigation indicated that a significant fraction—specifically 56% of conventional pharmaceuticals (particularly those functioning as Protein Kinase Inhibitors) fell outside Lipinski's limits [33].

The absorption of trametinib is significantly affected by food, as evidenced by Cox et al. [34], who demonstrated a reduction in absorption rate and extent with a high-fat meal. This finding emphasizes the clinical significance of administering trametinib on an empty stomach to ensure consistent and optimal drug levels. The absorption profiles of Trametinib, 1C, and 2R reveal uniformly low skin permeability, yet differ significantly in water solubility, wherein 2R displays enhanced solubility contrasted with the poor solubility of trametinib and 1C; notwithstanding their low solubility, both T
trametinib and 1C present high intestinal absorption, suggesting efficient absorption from the gastrointestinal tract. The achievement of 100% intestinal absorption by 2R, contrasting with the poor water solubility of trametinib and 1C, coupled with uniformly low skin permeability, indicates oral administration as the preferred route; furthermore, the superior water solubility of 2R suggests enhanced bioavailability and simplified formulation compared to the other compounds.

Despite variations in VDss, Fu, and BBB/CNS permeability, trametinib and 1C exhibit lower VDss and fraction unbound values, suggesting reduced tissue distribution and increased protein binding compared to 2R; however, limited BBB and CNS permeability across all compounds, indicated by negative log BB and log PS values, potentially restricts their therapeutic applications in central nervous system disorders.

The essential nature of cytochrome P450 interactions in drug pharmacokinetics is supported by investigations such as Patel et al. [35], which showed that P450 inhibitors and inducers, along with age, bilirubin concentration, and body weight, had a marked impact on the pharmacokinetic properties of selumetinib. Metabolic profiles of Table 5 demonstrate consistent CYP2C9 inhibition across all three compounds, requiring careful consideration of drug-drug interactions, particularly in combination regimens, while the absence of CYP1A2 and CYP2D6 inhibition suggests a lower likelihood of interactions with drugs metabolized by these specific enzymes.

Analysis of the total clearance values for Trametinib, 1C, and 2R demonstrates minor variations in their elimination rates, with total clearance, a measure of plasma volume cleared per unit time, serving as a critical parameter for determining dosing regimens, as it reflects the body's efficiency in drug removal. Despite slight variations in log total clearance, all three compounds demonstrate relatively low clearance rates, as evidenced by their negative log values; while trametinib and 1C exhibit slightly lower clearance than 2R, the overall similarity in elimination suggests that dosing regimens may require adjustments to maintain therapeutic concentrations and mitigate the risk of drug accumulation. However, the combination of high potency, selectivity, and a long circulating half-life in trametinib presents a promising approach for effectively navigating the anticipated limited therapeutic index associated with clinical MEK inhibitors [36].

The therapeutic utility of trametinib is restricted due to its adverse toxicity profile. Despite superior efficacy

in melanoma, the clinical application of the dabrafenib and trametinib combination is constrained by pyrexia-induced treatment interruptions [37]. Furthermore, the administration of trametinib in a phase 1 study resulted in dose-limiting toxicities such as rash, diarrhoea, and central serous retinopathy [31]. Additionally, in the management of pediatric low-grade gliomas, trametinib presents a promising therapeutic option. A recent investigation has demonstrated that therapeutic drug monitoring is crucial for enhancing treatment efficacy and reducing toxicity in this population, thereby advocating for patient-specific trametinib dosing strategies [38]. The analysis of LD50 and LOAEL values of Table 5 reveals that Trametinib, 1C, and 2R share comparable acute toxicity profiles, but 2R exhibits a significantly lower LOAEL, indicating a higher chronic toxicity potential and requiring careful clinical consideration of dosing and exposure duration, while trametinib and 1C suggest better chronic tolerability.

Pharmacokinetic analysis indicates that compound 2R demonstrates optimal intestinal absorption, an increased Vdss, and higher lipophilicity. Compared to trametinib, 2R exhibits pharmacokinetic properties that suggest improved efficacy. Although 2R shows higher toxicity, its superior overall profile warrants consideration as a potential replacement for trametinib, provided strategies are implemented to mitigate its toxic effects. Integrating the interaction profile and pharmacokinetic assessments, the evidence collectively highlights 2R as a compound with enhanced therapeutic potential.

Trametinib was recently examined in a phase I dose-escalation study involving 18 canine cancer subjects, which established an acceptable safety margin and yielded population pharmacokinetic data conducive to further clinical assessment [39]. Due to the shared biological characteristics between canine and human cancers, these studies yield translational data that can facilitate advancements in drug development for both human and veterinary medicine. The present study extends the active series of MEK1 inhibitors by designing and evaluating trametinib analogues with enhanced inhibitory potential, highlighting promising candidates for future therapeutic development in MEK-driven cancers.

4. CONCLUSION

In conclusion, the structure-activity relationships of trametinib were systematically examined to create a series with enhanced MEK1 binding affinity, refined interaction profiles, and optimized pharmacokinetic properties. Compound 2R emerged as a promising lead, exhibiting superior binding interactions and favorable pharmacokinetic characteristics compared to trametinib. These results underscore the value of computational drug discovery approaches in guiding the rational design of next-generation MEK inhibitors. By providing actionable translational insights, this work lays a strong foundation for subsequent experimental validation and the development of more effective targeted cancer therapies.

Declaration of Conflict of Interest

The authors declare no conflicts of interest

Funding Information

No funding received for this work.

Author Contribution

Conceptualization: S.S.U.; data collection: A.S.W; data interpretation: A.S.W; writing the first draft: A.S.W; Manuscript editing and reviewing: S.S.U; Project administration: S.S.U.

References

[1] P. Rutkowski, I. Lugowska, H. Kosela-Paterczyk, and K. Kozak, Trametinib: a MEK inhibitor for management of metastatic melanoma, OncoTargets and Therapy, 2251, 2015. DOI: 10.2147/ott.s72951.

[2] J. Zhu, C. Li, H. Yang, X. Guo, T. Huang, and W. Han, Computational Study on the Effect of Inactivating/Activating Mutations on the Inhibition of MEK1 by Trametinib, International Journal of Molecular Sciences, 21 (6), 2167, 2020. DOI: 10.3390/ijms21062167.

[3] C.F. Zheng and K.L. Guan, Cloning and characterization of two distinct human extracellular signal-regulated kinase activator kinases, MEK1 and MEK2, Journal of Biological Chemistry, 268 (15), 11435–11439, 1993. DOI: 10.1016/S0021-9258(18)82142-1.

[4] J.F. Ohren, H. Chen, A. Pavlovsky, C. Whitehead, E. Zhang, P. Kuffa, C. Yan, P. McConnell, C. Spessard, C. Banotai, W.T. Mueller, A. Delaney, C. Omer, J. Sebolt-Leopold, D.T. Dudley, I.K. Leung, C. Flamme, J. Warmus, M. Kaufman, and S. Barrett, Structures of human MAP kinase kinase 1 (MEK1) and MEK2 describe novel noncompetitive kinase inhibition, Nature Structural & Molecular Biology, 11 (12), 1192–1197, 2004. DOI: 10.1038/nsmb859.

[5] A. Bagheri, S.M.I. Moezzi, P. Mosaddeghi, S.N. Parashkouhi, S.M.F. Hoseini, F. Badakhshan, and M. Negahdaripour, Interferon-inducer antivirals: potential candidates to combat COVID-19, International Immunopharmacology, 107245, 2020. DOI: 10.1016/j.intimp.2020.107245.

[6] T. Yamaguchi, T. Yoshida, R. Kurachi, J. Kakegawa, Y. Hori, T. Nanayama, K. Hayakawa, H. Abe, K. Takagi, Y. Matsuzaki, M. Koyama, S. Yogosawa, Y. Sowa, T. Yamori, N. Tajima, and T. Sakai, Identification of JTP-70902, a $p15^{INK4b}$-inductive compound, as a novel MEK1/2 inhibitor, Cancer Science, 98 (11), 1809–1816, 2007. DOI: 10.1111/j.1349-7006.2007.00604.x.

[7] C.J.M. Wright and P.L. McCormack, Trametinib: First Global Approval, Drugs, 73 (11), 1245–1254, 2013. DOI: 10.1007/s40265-013-0096-1.

[8] C. Leonowens, C. Pendry, J. Bauman, G.C. Young, M. Ho, F. Henriquez, L. Fang, R.A. Morrison, K. Orford, and D. Ouellet, Concomitant oral and intravenous pharmacokinetics of trametinib, a MEK inhibitor, in subjects with solid tumours, British Journal of Clinical Pharmacology, 78 (3), 524–532, 2014. DOI: 10.1111/bcp.12373.

[9] P.K. Wu and J.I. Park, MEK1/2 Inhibitors: Molecular Activity and Resistance Mechanisms, Seminars in Oncology, 42 (6), 849–862, 2015. DOI: 10.1053/j.seminoncol.2015.09.023.

[10] R. Roskoski, Allosteric MEK1/2 inhibitors including cobimetanib and trametinib in the treatment of cutaneous melanomas, Pharmacological Research, 117, 20–31, 2017. DOI: 10.1016/j.phrs.2016.12.009.

[11] S.S. Uthumange, A. Jun, X.W. Chee, and K.Y. Yeong, Ringing medicinal chemistry: The importance of 3-membered rings in drug discovery, Bioorganic & Medicinal Chemistry, 117980, 2024. DOI: 10.1016/j.bmc.2024.117980.

[12] R. Roskoski, Classification of small molecule protein kinase inhibitors based upon the structures of their drug-enzyme complexes, Pharmacological Research, 103, 26–48, 2016. DOI: 10.1016/j.phrs.2015.10.021.

[13] G.R. Blumenschein, E.F. Smit, D. Planchard, D.W. Kim, J. Cadranel, T. De Pas, F. Dunphy, K. Udud, M.J. Ahn, N.H. Hanna, J.H. Kim, J. Mazieres, S.W. Kim, P. Baas, E. Rappold, S. Redhu, A. Puski, F.S. Wu, and P.A. Jänne, A randomized phase II study of the MEK1/MEK2 inhibitor trametinib (GSK1120212) compared with docetaxel in KRAS-mutant advanced non-small-cell lung cancer (NSCLC), Annals of Oncology: Official Journal of the European Society for Medical Oncology, 26 (5), 894–901, 2015. DOI: 10.1093/annonc/mdv072.

[14] C. Lorimer, L. Cheng, R. Chandler, K. Garcez, V. Gill, K. Graham, W. Grant, S. Sardo Infirri, J. Wadsley, L. Wall, N. Webber, K.H. Wong, and K. Newbold, Dabrafenib and Trametinib Therapy for Advanced Anaplastic Thyroid Cancer – Real-World Outcomes From UK Centres, Clinical Oncology, 35 (1), e60–e66, 2022. DOI: 10.1016/j.clon.2022.10.017.

[15] É. Bouffet, J.R. Hansford, M.L. Garrè, J. Hara, A. Plant-Fox, I. Aerts, F. Locatelli, J.L. Papusha, F. Sahm, U. Tabori, K.J. Cohen, R.J. Packer, O. Witt, L. Sandalic, A. Bento, M.W. Russo, and D. Hargrave, Dabrafenib plus Trametinib in Pediatric Glioma with $BRAF^{V600}$ Mutations, The New England Journal of Medicine, 389 (12), 1108–1120, 2023. DOI: 10.1056/nejmoa2303815.

[16] V. Subbiah, R.J. Kreitman, Z.A. Wainberg, A. Gazzah, U. Lassen, A. Stein, P.Y. Wen, S. Dietrich, A. de Jonge, J.Y. Blay, A. Italiano, K. Yonemori, D.C. Cho, F. de Vos, P. Moreau, E. Elez, J.H.M. Schellens, C.C. Zielinski, S. Redhu, and A. Boran, Dabrafenib plus trametinib in $BRAF^{V600E}$-mutated rare cancers: the phase 2 ROAR trial, Nature Medicine, 29 (5), 1103–1112, 2023. DOI: 10.1038/s41591-023-02321-8.

[17] Y. Zhao and A.A. Adjei, The clinical development of MEK inhibitors, Nature Reviews Clinical Oncology, 11 (7), 385–400, 2014. DOI: 10.1038/nrclinonc.2014.83.

[18] G.M. Morris, R. Huey, W. Lindstrom, M.F. Sanner, R.K. Belew, D.S. Goodsell, and A.J. Olson, AutoDock4 and AutoDockTools4: Automated docking with selective receptor flexibility, Journal of Computational chemistry, 30 (16), 2785–2791,

2009. DOI: 10.1002/jcc.21256.
[19] S. Hashemzadeh, F. Ramezani, and H. Rafii-Tabar, Study of Molecular Mechanism of the Interaction Between MEK1/2 and Trametinib with Docking and Molecular Dynamic Simulation, Interdisciplinary Sciences: Computational Life Sciences, 11 (1), 115–124, 2018. DOI: 10.1007/s12539-018-0305-4.
[20] W. Humphrey, A. Dalke, and K. Schulten, VMD: Visual molecular dynamics, Journal of Molecular Graphics, 14 (1), 33–38, 1996. DOI: 10.1016/0263-7855(96)00018-5.
[21] Z.M. Khan, A.M. Real, W.M. Marsiglia, A. Chow, M.E. Duffy, J.R. Yerabolu, A.P. Scopton, and A.C. Dar, Structural basis for the action of the drug trametinib at KSR-bound MEK, Nature, 588 (7838), 509–514, 2020. DOI: 10.1038/s41586-020-2760-4.
[22] A. Daina, O. Michielin, and V. Zoete, SwissADME: a Free Web Tool to Evaluate pharmacokinetics, drug-likeness and Medicinal Chemistry Friendliness of Small Molecules, Scientific Reports, 7 (1), 1–13, 2017. DOI: 10.1038/srep42717.
[23] D.E.V. Pires, T.L. Blundell, and D.B. Ascher, pkCSM: Predicting Small-Molecule Pharmacokinetic and Toxicity Properties Using Graph-Based Signatures, Journal of Medicinal Chemistry, 58 (9), 4066–4072, 2015. DOI: 10.1021/acs.jmedchem.5b00104.
[24] H. Park, S. Lee, and S. Hong, Discovery of MEK/PI3K dual inhibitor via structure-based virtual screening, Bioorganic & Medicinal Chemistry Letters, 22 (15), 4946–4950, 2012. DOI: 10.1016/j.bmcl.2012.06.041.
[25] R.A. Heald, P. Jackson, P. Savy, M. Jones, E. Gancia, B. Burton, R. Newman, J. Boggs, E. Chan, J. Chan, E. Choo, M. Merchant, P. Rudewicz, M. Ultsch, C. Wiesmann, Q. Yue, M. Belvin, and S. Price, Discovery of Novel Allosteric Mitogen Activated Protein Kinase Kinase (MEK) 1,2 Inhibitors Possessing Bidentate Ser212 Interactions, Journal of Medicinal Chemistry, 55 (10), 4594–4604, 2012. DOI: 10.1021/jm2017094.
[26] L. Palmieri and G. Rastelli, αC helix displacement as a general approach for allosteric modulation of protein kinases, Drug Discovery Today, 18 (7-8), 407–414, 2012. DOI: 10.1016/j.drudis.2012.11.009.
[27] H. Tecle, J. Shao, Y. Li, M. Kothe, S. Kazmirski, J. Penzotti, Y.-H. Ding, J. Ohren, D. Moshinsky, R. Coli, N. Jhawar, E. Bora, S. Jacques-O'Hagan, and J. Wu, Beyond the MEK-pocket: Can current MEK kinase inhibitors be utilized to synthesize novel type III NCKIs? Does the MEK-pocket exist in kinases other than MEK?, Bioorganic & Medicinal Chemistry Letters, 19 (1), 226–229, 2009. DOI: 10.1016/j.bmcl.2008.10.108.
[28] M.R. Scholfield, C.M.V. Zanden, M. Carter, and P.S. Ho, Halogen bonding (X-bonding): A biological perspective, Protein Science, 22 (2), 139–152, 2012. DOI: 10.1002/pro.2201.
[29] F. Zou, Y. Yang, T. Ma, J. Xi, J. Zhou, and X. Zha, Identification of novel MEK1 inhibitors by pharmacophore and docking based virtual screening, Medicinal Chemistry Research, 26 (4), 701–713, 2017. DOI: 10.1007/s00044-017-1788-y.
[30] I. Almi, S. Belaidi, N. Melkemi, and D. Bouzidi, Chemical Reactivity, Drug-Likeness and Structure Activity/Property Relationship Studies of 2,1,3-Benzoxadiazole Derivatives as Anti-Cancer Activity, Journal of Bionanoscience, 12 (1), 49–57, 2018. DOI: 10.1166/jbns.2018.1503.
[31] J.R. Infante, L.A. Fecher, G.S. Falchook, S. Nallapareddy, M.S. Gordon, C. Becerra, D.J. DeMarini, D.S. Cox, Y. Xu, S.R. Morris, V.G. Peddareddigari, N.T. Le, L. Hart, J.C. Bendell, G. Eckhardt, R. Kurzrock, K. Flaherty, H.A. Burris, and W.A. Messersmith, Safety, pharmacokinetic, pharmacodynamic, and efficacy data for the oral MEK inhibitor trametinib: a phase 1 dose-escalation trial, The Lancet Oncology, 13 (8), 773–781, 2012. DOI: 10.1016/s1470-2045(12)70270-x.
[32] C.A. Lipinski, F. Lombardo, B.W. Dominy, and P.J. Feeney, Experimental and computational approaches to estimate solubility and permeability in drug discovery and development settings, Advanced Drug Delivery Reviews, 23 (1-3), 3–25, 1997. DOI: 10.1016/s0169-409x(96)00423-1.
[33] F. Carles, S. Bourg, C. Meyer, and P. Bonnet, PKIDB: A Curated, Annotated and Updated Database of Protein Kinase Inhibitors in Clinical Trials, Molecules, 23 (4), 908, 2018. DOI: 10.3390/molecules23040908.
[34] D.S. Cox, K. Papadopoulos, L. Fang, J. Bauman, P. LoRusso, A. Tolcher, A. Patnaik, C. Pendry, K. Orford, and D. Ouellet, Evaluation of the effects of food on the single-dose pharmacokinetics of trametinib, a first-in-class MEK inhibitor, in patients with cancer, Journal of Clinical Pharmacology, 53 (9), 946–954, 2013. DOI: 10.1002/jcph.115.
[35] P. Patel, E. Howgate, P. Martin, D.J. Carlile, L. Aarons, and D. Zhou, Population pharmacokinetics of the MEK inhibitor selumetinib and its active N-desmethyl metabolite: data from 10 phase I trials, British Journal of Clinical Pharmacology, 84 (1), 52–63, 2017. DOI: 10.1111/bcp.13404.
[36] A.G. Gilmartin, M.R. Bleam, A. Groy, K.G. Moss, E.A. Minthorn, S.G. Kulkarni, C.M. Rominger, S. Erskine, K.E. Fisher, J. Yang, F. Zappacosta, R. Annan, D. Sutton, and S.G. Laquerre, GSK1120212 (JTP-74057) is an inhibitor of MEK activity and activation with favorable pharmacokinetic properties for sustained in vivo pathway inhibition, Clinical Cancer Research: An Official Journal of the American Association for Cancer Research, 17 (5), 989–1000, 2011. DOI: 10.1158/1078-0432.CCR-10-2200.
[37] H.Y. Kim, J.K. Duong, M. Gonzalez, G.V. Long, A.M. Menzies, H. Rizos, S.Y. Lim, J. Lee, and A.V. Boddy, Pharmacokinetic

and cytokine profiles of melanoma patients with dabrafenib and trametinib-induced pyrexia, Cancer Chemotherapy and Pharmacology, 83 (4), 693–704, 2019. DOI: 10.1007/s00280-019-03780-y.

[38] L. Pagnot, I. Granger, J. Guitton, B. Favier, A. Ceraulo, C. Faure-Conter, P. Leblond, and M. Philippe, Real-world pharmacokinetics of trametinib in pediatric low-grade glioma, Cancer Chemotherapy and Pharmacology, 95 (1), 2025. DOI: 10.1007/s00280-025-04761-0.

[39] M. Takada, K. Kitagawa, Y. Zhang, J. B. Bulitta , S. Moirano, A. Jones, J. Borgen, A. Onsager, T. Thaiwong, D. Vail, Population Pharmacokinetics, Pharmacodynamics and Safety Properties of Trametinib in Dogs With Cancer: A Phase I Dose Escalating Clinical Trial, Veterinary and Comparative Oncology, 22(3), 410–421, 2024. doi:https://doi.org/10.1111/vco.12989.